

The Use of FFT Method in Geoid Modelling

Wan Abdul Aziz bin Wan Mohd. Akib, Ph.D
Centre for Geodetic & Geodynamic Studies
Faculty of Geoinformation Science & Engineering
Universiti Teknologi Malaysia
Skudai, 80990

Abstract

The paper presents the spectral method known as Fast Fourier Transform (FFT) to compute discrete convolution integrals. Geoid heights are computed by reformulating the Stokes' equation in convolution form and using gridded residual gravity anomalies as input data. Discrete spectra of the kernel functions are used for the geoid heights appending simultaneously zero-padding around the input gravity matrix in order to avoid circular convolution effects. This procedure provides identical results to those from the rigorous numerical integration. The computed quantities are compared to a set of geoid heights derived from a contribution of GPS traverse with levelled orthometric heights.

1.0 INTRODUCTION

Nowadays, the geoid heights covering a national territory are considered of very important information which should be available to users of applied geodesy, geophysics and other branches of geosciences and ocean sciences. Among others, a detailed geoid representation fulfills some of the requirements for a definition of a national vertical datum. Nowadays, with the rapid expansion of applications of the GPS positioning and the improvement of positioning accuracy, there is a need for gravimetric geoid of high accuracy for GPS-levelling, i.e. GPS-derived orthometric heights. Rigorously, the geoid is defined as an equipotential surface of the earth's gravity field corresponding to the mean sea level, see Figure: 1.0.

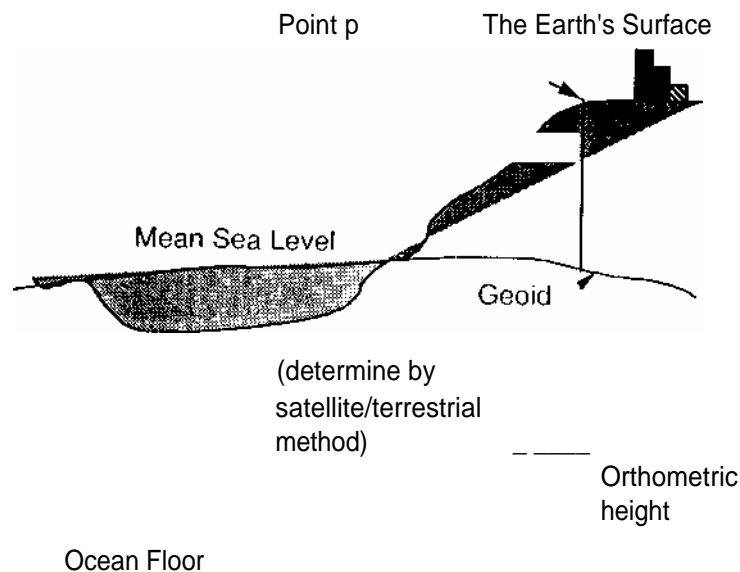


Figure: 1.0 - Geoid and Mean Sea Level.

The problem of geoid determination may be viewed in the wider context of geodetic gravity field modelling, i.e. given some quantities - 'observations' of the earth's gravity field, what are the other quantities - 'prediction'. This boundary value problem deals with the determination of potential,

harmonic outside the masses, from gravity anomalies given everywhere on the geoid surface. The geoid height can be determined using the following expression (Heiskanen and Moritz, 1967):

$$N = \frac{R}{g} \Delta g \quad \dots(1)$$

where $d\sigma$ is the element of unit sphere, Δg is the gravity anomaly, R is the radius of the earth and $S(\psi)$ is Stokes' function given by:

$$S(\psi) = \frac{1}{\sin(\frac{\psi}{2})} - 6\sin\frac{\psi}{2} + 1 - 5\cos\psi - 3\cos\psi \ln(\sin\frac{\psi}{2} + \sin^2\frac{\psi}{2}) \quad \dots(2)$$

ψ is the spherical distance between the data point (ϕ, λ) and the prediction point (ϕ_p, λ_p) .

In principle, equation (1) can be approximated by a series expansion of spherical harmonic coefficients which is referred to the *Geodetic Reference System 1980* (GRS80). The solution is called *geopotential model solution* (N_{GM}):

$$N_{GM} = \frac{KM}{\gamma R} \sum_{n=2}^{n_{max}} \sum_{m=0}^{m=n} P_{nm} \cos\phi (C_{nm} \cos m\lambda + S_{nm} \sin m\lambda) \quad \dots(3)$$

where C_{nm}, S_{nm} are the fully normalized geopotential coefficients;
 P_{nm} is the Legendre function;
 K is the Newton's Gravitational Constant; and
 M is the mass of the earth.

The geopotential model solution forms the basis for all local approximation of the gravity field, i.e. to provide the long to medium wavelength of the gravity field spectrum. It should be noted that for local geoid modelling, the gravity anomalies used with Stokes' integral in equation (1) contain the contributions for the topography (short/very short wavelength of the gravity field spectrum), especially in the mountainous regions. In practice, therefore, the procedure of local geoid modelling involves the remove stage (pre-processing) and the restoration stage (post-processing) of the topographic and geopotential model contributions as follows:

$$\Delta g = \Delta g_{\text{free-air}} - \Delta g_{\text{geopotential model}} - \Delta g_{\text{topo}} \quad \Rightarrow \quad \text{Remove stage} \quad \dots(4)$$

$$N = N_{\text{geopotential model}} + N_{\text{gravity}} + N_{\text{topo (indirect effect)}} \quad \Rightarrow \quad \text{Restoration stage} \quad \dots(4a)$$

The modelling procedure for local geoids can be implemented by using Stokes' integral (space domain numerical integration), Least Squares Collocation (LSC), Point Mass Fitting or Spectral method. This paper highlights some basic algorithms of the spectral method which is known as *Fast Fourier Transform (FFT)* and its evaluation of Stokes' integral for gravimetric geoid determination.

2.0 THE NEED FOR SPECTRAL TECHNIQUES

Due to the fact that it is very time consuming to evaluate Stokes' integral, it is often attempted to reduce the size of the area by modifying the Stokes' kernel function. The basic idea, was first presented by Molodensky et.al. (1962) which reduces the truncation error by a suitable modification of Stokes kernel, and this approach was implemented in Vanicek and Sjöberg (1989) and Featherstone (1993). Truncation error is the error caused by limiting the area of the integration of the terrestrial gravity anomalies to a spherical cap.

The LSC method which is theoretically sounds unfortunately suffers from practical disability since it generates a system of equations of order equal to the number of observation points. This kind of method increases the requirements of the computing resources especially when the data volume increased dramatically, both in quantity and in type. The applications of the LSC method requires the choice of a *reproducing kernel*, that is a local covariance function. As a matter of fact, the implementation of the LSC method relies fundamentally on the capacity of modelling a suitable

One of the basic properties of the 2-D Fourier transform is the *convolution (frequency domain convolution)* of the two functions, denoted by symbol $*$:

$$h(x,y) * g(x,y) \leftrightarrow H(u,v) G(u,v) \quad \text{or} \quad h(x,y)g(x,y) \leftrightarrow H(u,v) * G(u,v) \quad \dots(11)$$

The simple spectral representation of the above equation is of great practical importance. In general, the process involves two direct and one inverse Fourier transforms :

$$x(t) = g(t) * h(t) \quad \dots(12)$$

$$= F^{-1}[F(g(t))F(h(t))] \quad \dots(12a)$$

where t is time (periodic with period T which can be related to frequency $\Delta\omega=2\pi/T$) or, usually distance in geodetic applications.

In practice, the estimation of the spectrum in a finite area (say $-X/2 \leq x \leq X/2$, $-Y/2 \leq y \leq Y/2$) can only be obtained by the finite integral. Therefore, equations (5) can be rewritten as:

$$H_F(u,v) = \int_{-X/2}^{X/2} \int_{-Y/2}^{Y/2} h_F(x,y) e^{-2\pi i(ux+vy)} dx dy \quad \dots(13)$$

Since the data are assumed to be known only at a discrete points of a regular grid with sampling interval $\Delta x, \Delta y$ then the record lengths may thus be expressed by :

$$X = M\Delta x, \quad Y = N\Delta y \quad \dots(14)$$

where M and N are the number of points along the x and y directions, respectively.

With the discrete given data, the spectral estimation integral of equation (13) may now be approximated by a sum of:

$$H_D(u_m, v_n) = \sum_{k=0}^{M-1} \sum_{l=0}^{N-1} h(x_k, y_l) e^{-2\pi i(u_m x_k + v_n y_l)} \Delta x \Delta y \quad \dots(15)$$

where $m = 0, 1, 2, \dots, M-1$, $n = 0, 1, 2, \dots, N-1$.

Assuming the data to be periodically extended in the plane, the spectrum becomes discrete with frequency spacings, see Figure: 2.0.

$$\Delta u = \frac{1}{X} = \frac{1}{M\Delta x}, \quad \Delta v = \frac{1}{Y} = \frac{1}{N\Delta y} \quad \dots(16)$$

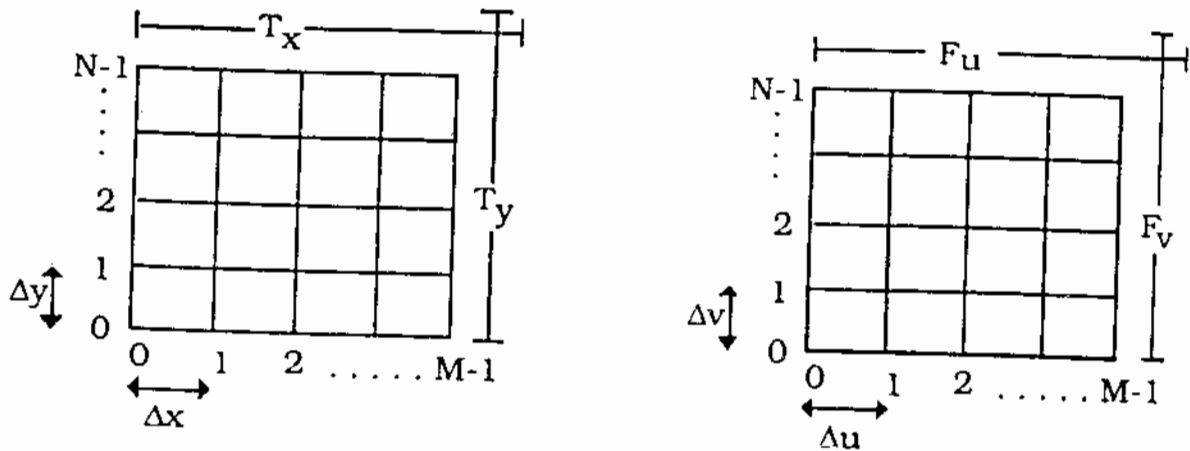


Figure: 2.0 - The Relationship between space domain and frequency domain

Therefore, in terms of a discrete Fourier transform pair, the spectral transformations may be written as:

$$H(m\Delta u, n\Delta v) = \Delta x \Delta y \sum_{k=0}^{M-1} \sum_{l=0}^{N-1} h(k\Delta x, l\Delta y) \exp\left(-2\pi i \left(\frac{mk}{M} + \frac{nl}{N}\right)\right) \quad \text{.....(17)}$$

$$h(k\Delta x, l\Delta y) = \Delta u \Delta v \sum_{m=0}^{M-1} \sum_{n=0}^{N-1} H(m\Delta u, n\Delta v) \exp\left(-2\pi i \left(\frac{mk}{M} + \frac{nl}{N}\right)\right) \quad \text{.....(18)}$$

where k, l, m and n are the integer wavenumbers; $m = 0, 1, 2, \dots, M-1$; $n = 0, 1, 2, \dots, N-1$;
 $k = 0, 1, 2, \dots, M-1$; $l = 0, 1, 2, \dots, N-1$

This is the basic form of the FFT algorithm used to evaluate the Discrete Fourier Transform (DFT). Here, the FFT is an algorithm for computing the DFT much faster (number of required complex multiplications proportional to $N \log_2 N$) than by the conventional Fourier transform (number of required complex multiplications proportional to N^2). To illustrate the FFT algorithm, the intuitive development presented in Brigham (1988) for 1-D FFT is given in Appendix I.

4.0 STOKES' INTEGRAL IN THE FREQUENCY DOMAIN

The contribution of the gravity anomalies can be computed in variety of ways. For a small distances inside the area of integration, the planar approximation of Stokes' Integral can be used where the first term of $S(\psi)$ in equation (2) being the dominant one. Using the planar distance l , where $l = R\psi$, then equation (1) is reduced to:

$$\frac{1}{\sin(\frac{\psi}{2})} \approx \frac{2}{\psi} \approx \frac{2R}{l} \quad \text{.....(19)}$$

If we use rectangular coordinate instead of polar coordinate to describe the area of integration, we have:

$$R^2 d\sigma = dx dy \quad \text{.....(20)}$$

Thus, equation (1) can be rewritten as:

$$N_{(x_p, y_p)} = \frac{1}{2\pi\gamma} \iint_A \frac{\Delta g(x, y)}{l} dx dy \quad \text{.....(21)}$$

$$l = [(x - x_p)^2 + (y - y_p)^2]^{1/2} \quad \text{.....(22)}$$

where x, y are the coordinates of the data points and x_p, y_p are the coordinates of the computation point.

Now, with respect to the properties of the Fourier transform given by equations (12) and (12a), the above equation can also be formulated as 2-D convolution integral :

$$N = \frac{1}{2\pi\gamma} \Delta g(x_p, y_p) * l_N(x_p, y_p) \quad \text{.....(23)}$$

where l_N is the planar form of Stokes' kernel function, given by:

$$l_N(x, y) = (2\pi)^{-1} (x^2 + y^2)^{-1/2} \quad \text{.....(24)}$$

Consequently, equation (23) can be evaluated as follows:

$$N = \frac{1}{2\pi\gamma} \{F^{-1}(F(\Delta g(x_p, y_p))F(l_N(x_p, y_p)))\} \quad \text{.....(25)}$$

$$= \frac{1}{2\pi\gamma} F^{-1}(\Delta G(u, v) L_N(u, v)) \quad \text{.....(25a)}$$

4.1 Point Gravity Anomalies as Input Data

Using $(M \times N)$ gridded point anomalies with spacing $(\Delta x, \Delta y)$ the geoid height of a point (x_k, y_l) can be estimated by the following discrete convolution:

$$N = \frac{1}{2\pi\gamma} \sum_{i=0}^{M-1} \sum_{j=0}^{N-1} \Delta g(x_i, y_j) l_N(x_k - x_i, y_l - y_j) \Delta x \Delta y \quad \text{.....(26)}$$

where l_N is the inverse geometrical distance between the points $(j-k)$ and $(j-l)$.

$$l_N(x_k - x_i, y_l - y_j) = \begin{cases} ((x_k - x_i)^2 + (y_l - y_j)^2)^{-1/2}, & x_k \neq x_i, y_l \neq y_j \\ 0, & x_k = x_i, y_l = y_j \end{cases} \quad \text{.....(27)}$$

The geoid heights can then be evaluated by the FFT as follows:

$$N = \frac{1}{2\pi\gamma} F^{-1}(\Delta G(u_m, v_n) L_N(u_m, v_n)) \quad \text{.....(28)}$$

ΔG has to be computed by the DFT of equation (17):

$$\Delta G(u_m, v_n) = F(\Delta g(x_k, y_l)) = \sum_{k=0}^{M-1} \sum_{l=0}^{N-1} \Delta g(x_k, y_l) e^{-i2\pi(\frac{mk}{M} + \frac{nl}{N})} \Delta x \Delta y \quad \text{.....(29)}$$

and $L_N(u_m, v_n)$ can be evaluated by :

$$L_N(u_m, v_n) = F(l_N(x_k, y_l)) = \sum_{k=0}^{M-1} \sum_{l=0}^{N-1} l_N(x_k, y_l) e^{-i2\pi(\frac{mk}{M} + \frac{nl}{N})} \Delta x \Delta y \quad \text{.....(30)}$$

4.2 Mean Gravity Anomalies as Input Data

If the input data are $(M \times N)$ gridded mean anomalies Δg , the planar Stokes formula can be formulated as:

$$N = \frac{1}{2\pi\gamma} \sum_{i=0}^{M-1} \sum_{j=0}^{N-1} \Delta g(x_i, y_j) \bar{l}_N(x_k - x_i, y_l - y_j) \quad \text{.....(31)}$$

where \bar{l}_N is the mean Stokes kernel spectrum given by

$$\bar{l}_N = x \ln(y + (x^2 + y^2)^{1/2}) + y \ln(x + (x^2 + y^2)^{1/2}), \begin{vmatrix} x_k + \Delta x / 2 & y_l + \Delta y / 2 \\ x_k - \Delta x / 2 & y_l - \Delta y / 2 \end{vmatrix} \quad \text{.....(32)}$$

Equation (31) can also be efficiently evaluated via FFT:

$$N = \frac{1}{2\pi\gamma} F^{-1} \{ F(\Delta g(x_k, y_l)) F(\bar{l}_N(x_k - y_l)) \} \quad \text{.....(33)}$$

or

$$N = \frac{1}{2\pi\gamma} F^{-1}(\Delta G(u_m, v_n) \bar{L}_N(u_m, v_n)) \quad \text{.....(33a)}$$

Details of the implementation of the above formulas can be found in Sideris and Tziavos (1988).

5.0 CIRCULAR CONVOLUTION AND EDGE EFFECTS

In the practical implementation of the Fourier formulas, usually there are two approximations employed:

- (a) Continuous integration are replaced by discrete summations, and
- (b) The infinite limits of summation are replaced by finite one

Discretization of equation (12) for both functions $g(t)$ and $h(t)$ at N points results in the following expression:

$$x(k) = \sum_{l=0}^{N-1} g(l)h(k-l)\Delta t = g(k) * h(k) \quad \text{.....(34)}$$

where Δt is the time spacing which can be related to frequency spacing $\Delta\omega$ and the numbers of discrete points N as $1/\Delta\omega = N\Delta t$. In practice, N is much easier to control than Δt but it will always be a finite number and the leakage effect will always be present.

When the above equation is evaluated by numerical summation, the results is correct and correspond to linear convolution. If, however the discrete forms of equation (12a) is used instead, i.e.

$$x_p(k) = F^{-1}\{F(g_p(k))F(h_p(k))\} \quad \text{.....(35)}$$

The above function is treated as periodic (subscript p), the results are incorrect and correspond to circular convolution (Oppenheim and Schaffer, 1989). Hence, the equation (34) indicate that if $g(k)$ and $h(k)$ have N values each, the $x(k)$ will have $2N-1$ value. On the other hand, when equation (35) is evaluated by the (periodic) DFT, it is clear that the resulting $x(k)$ will has N values and will be periodic, as well. Mathematically, convolution can be viewed as linear convolutions contaminated by aliasing. Therefore, it should be noted that Stokes' formula is mathematically expressed by linear convolutions (equation 23) while most FFT algorithms are designated for the computation of circular convolutions, (ibid). Obviously, such approximation will introduced errors due to the truncation of the series that may be significant for the properties of the transformed functions. Distortion of the results will occur due to edge effects introduced by using the circular convolution instead of the linear convolution, see Figure: 3.0.

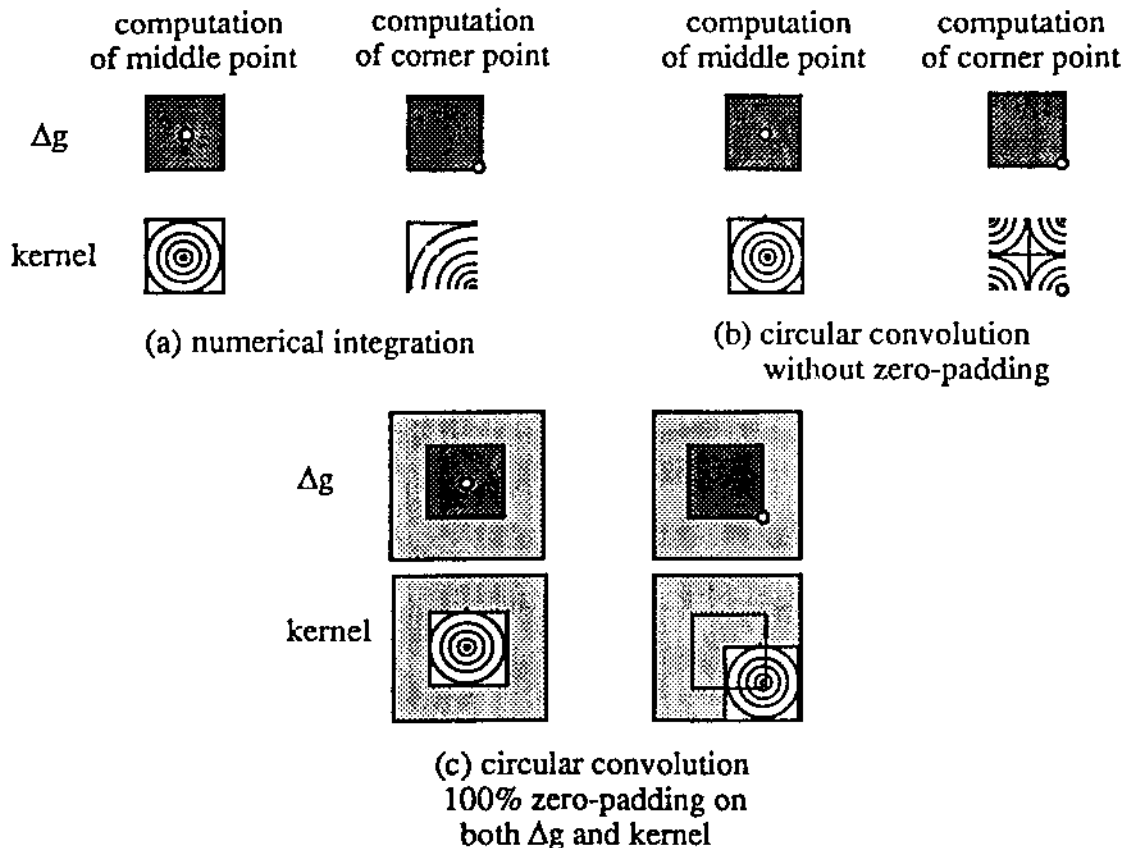


Figure: 3.0 - Edge effect and circular convolution in FFT evaluations of Stokes' Integral

Figure 3.0 illustrates the effect of circular convolution when the computation point is either at the centre or at a corner of the computational area. The small circle represents the computation point for the geoid height and at the same time, the maximum kernel function value. Figure 3(a) shows the correct kernel function corresponding to the numerical integration whereas Figure: 3(b) gives mirrored kernel function of the circular convolutions. When the computation point is not at the centre, it can be seen that the periodically mirrored kernel function values are not correct. One way of eliminating the edge effect is to append 100% zeros at each row and column of both convolved function, (Bracewell, 1986). In other words, zeros are appended to $g(k)$ and $h(k)$ in equation (36) as follows:

$$g'(k) = \begin{cases} g(k), 0 \leq k < N \\ 0, N \leq k < 2N \end{cases} \quad \text{.....(37)}$$

$$h'(k) = \begin{cases} h(k), 0 \leq k < N \\ 0, N \leq k < 2N \end{cases} \quad \text{.....(37a)}$$

In practice, the values of the kernel functions are computed at both the data points and the zero-padded points. The applications of zeros-padding around the gravity anomalies provides identical results with those obtained by the space domain integration, see Figure: 3(a) and Figure: 3(c).

6.0 NUMERICAL RESULTS

For the computation of the geoid heights, a set of surface mean 5'x5' free-air gravity anomalies in a 4°x4° area bounded by the limits $48^\circ \leq \phi \leq 52^\circ$ N, $235^\circ \leq \lambda \leq 239^\circ$ W. These gravity data values are referred to the GRS80 and have been reduced to the surface implied by the OSU91A geopotential model and topographic contributions, (Tziavos, Private Comm.). The contribution of the such derived residual gravity anomalies (removing stage) to geoid heights was computed and then to these residual geoid values, the contributions of the geopotential model and indirect effect were added (restoration stage). To assess the quality of the spectral method, the computed geoids (with and without the application of zeros-padding) are compared with those obtained by space numerical integration. The statistics found for the different residual geoid solutions is summarized in Table 1.0.

	PLANAR		FFT	
	ZERO		PADDING	
	NO		YES	
No. of Point	1296		1296	
Mean (m)	-0.26		-0.10	
Std.Dev. (m)	± 0.34		± 0.29	
Rms(m)	0.42		0.31	

Table: 1.0 - Statistical results of comparison of geoid heights derived from numerical integration and planar FFT

From Table: 1.0, it can be seen that the FFT computations can be improved by using discrete spectra for the kernels in combination with zeros-padding. As mentioned in Section 3.0, the application of zeros-padding therefore significantly reduced the effect of circular convolution. The geoid height differences derived from numerical integration and planar FFT (with zeros-padding) is plotted for a central part of the test area, see Figure: 4.0.

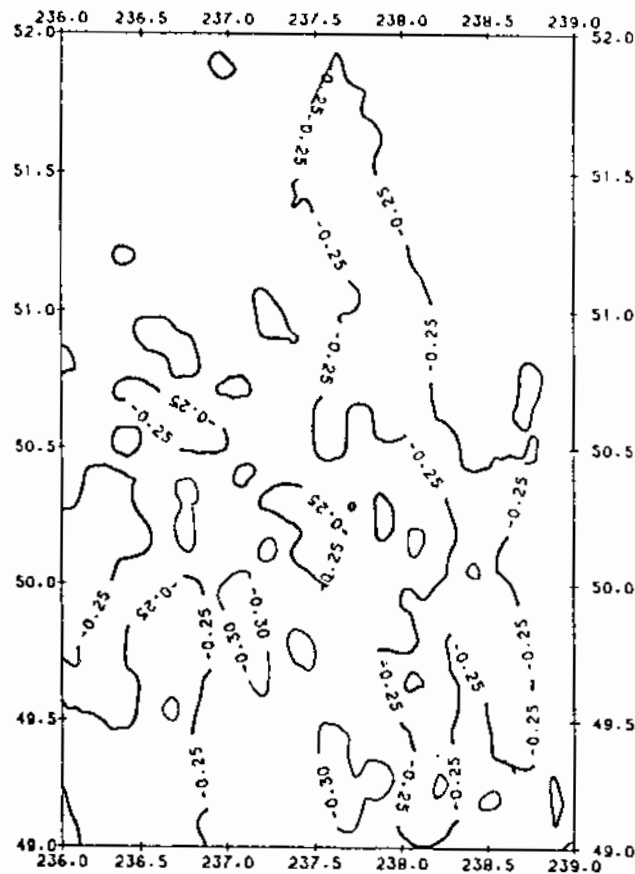


Figure: 4.0 - Geoid height differences between Numerical Integration and FFT

In the second numerical test, the relative geoid heights obtained by the FFT technique (with and without zeros-padding) are compared with corresponding heights derived from GPS ellipsoidal heights and orthometric heights. The GPS traverse in the test area is a approximately 180km long traverse consisting of 19 stations. The geoid heights on the 19 control stations of the GPS traverse derived by a bilinear interpolation technique. The results from this experiment are summarized in Table: 2.0.

	NUMERICAL INTEGRATION	PLANAR		FFT
		ZEROS		PADDING
		NO		YES
No.	18	18		18
Mean (m)	-0.28	-0.35		-0.34
Std.Dev. (m)	± 0.48	± 0.48		± 0.45
Rms (m)	0.54	0.59		0.55

Table: 2.0 - Comparison of relative geoid height derived from numerical integration and FFT method with respect to 19 controls stations of the GPS traverse

From the numerical tests for geoid heights performed in this study it appears that the FFT method with zeros-padding offers slightly better results compared to non-zero-padding solution. It is interesting to note that the results from the numerical integration is quite identical with those from FFT zeros-padding. The use of zeros-padding in small areas is still necessary to obtain best results. It showed that no additional errors will be brought into the results when the FFT method used from the evaluation of gravity field convolutions.

7.0 CONCLUDING REMARKS

The integral of the form of equation (11) are called convolution integral of the two functions and lend themselves to be evaluated by the FFT algorithms. The main advantage of the FFT method is that they can efficiently handle heterogeneous and noisy gridded data and give results of all grid points simultaneously which has made them a standard and is dispensable tool for geoid computations. Thus, the spectral techniques based on the FFT algorithms overcome very successfully the problem of slow computation speed, and provide a homogeneous coverage of results which are very suitable for interpolation and plotting purposes. There are some problems that effect the accuracy of the results and are usually believed to be unique to the FFT method. Actually, many of these problems such as aliasing and leakage effects are common to all methods (e.g. LSC, Numerical Integration) using the same data. For example, aliasing effects can be minimised by removing the high frequency information from topographic reduction to gravity anomalies. Similarly, the leakage effects can also be minimised by removing the low frequency information from the geopotential model coefficients.

The problem that are indeed unique to spectral method only include edge effect or circular convolution. The 100% zeros-padding technique can be used to eliminate the circular convolution and appears to provide identical results with those from the space domain numerical integration. Consequently, it seem not necessary to modify Stokes' kernel function which becomes even more obvious when the remove-restore technique (equations 4a and 4b) is used. Therefore, the FFT algorithms represent a very attractive alternative to the classical, time consuming approaches, provided gridded data are available.

REFERENCES

- Bracewell, R., (1986) : The Fourier Transform and Its Applications, 2nd. ed., revised, 444 pp., McGraw-Hill, New York.
- Brigham, E., (1988) : The FFT and Its Applications, Prentice Hall, Eaglewood Cliffs, New Jersey.
- Featherstone, (1993) : A GPS Controlled Gravimetric Determination of the Geoid of the British Isles
Ph.D Thesis, University of Newcastle Upon-Tyne, UK.
- Heiskanen and Moritz, (1967) : Physical Geodesy, W.H.Freeman and Co., San Francisco.
- Molodenskii, M, Eremeev, V. and Yurkina, M., (1962) : Methods for the Study of the Gravitational Field of the Earth.. Translated from Russian (1960), *Israel Program for Scientific Translation, Jerusalem.*
- Oppenheim, A.V, and Schafer, R.W., (1989) : Discrete Time Signal Processing, Prentice Hall, Eaglewood Cliffs, New Jersey
- Popoulis, A., (1977) : Signal Analysis, McGraw Hill, New York.
- Schwarz, K.P., M.G.Sideris and Forsberg, R., (1990) : The use FFT Techniques in Physical Geodesy, *Geophys.J.Int.*, 100, 485-514.
- Sideris, M.G. and Tziavos, I.N., (1988) : FFT Evaluation and Applications of Gravity Field Convolution Integrals with Mean and Points Data. *Bulletin Geodesique, Vol. 65, pp 521-540.*
- Vanicek, P and Sjoberg, L.F., (1989) : Kernel Modification in Generalised Stokes' Technique for Geoid Determination. In *Proc. of the IAG General Meeting, Edinburgh, August, 3-12.*
- Wan, A.A., (1994) : The Analysis of the Synthetic Covariance Functions for the Gravity Field Modelling Using LSC method. *Unpublished Report, Dept. of Photog. and Surv. Uni. Coll. London, UK.*

APPENDIX I

Suppose that the DFT of a function $f(k)$ with $N=4$ is required. Omitting, for simplicity, the constants in front of the summation symbol, we have

$$H(m) = \sum_{k=0}^{N-1} h(k) e^{-i2\pi km/N} = \sum_{k=0}^{N-1} h(k) W^{km} \quad , m=0, 1, 2, 3, \quad \dots(1)$$

or, equivalently,

$$\begin{bmatrix} H(0) \\ H(1) \\ H(2) \\ H(3) \end{bmatrix} = \begin{bmatrix} W^0 & W^0 & W^0 & W^0 \\ W^0 & W^1 & W^2 & W^3 \\ W^0 & W^2 & W^4 & W^6 \\ W^0 & W^3 & W^6 & W^9 \end{bmatrix} \begin{bmatrix} h(0) \\ h(1) \\ h(2) \\ h(3) \end{bmatrix} \quad \dots(2)$$

Since,

$$W^{km} = e^{-i2\pi km/N} = W^{km \bmod(N)} \quad \dots(3)$$

$$\begin{bmatrix} H(0) \\ H(1) \\ H(2) \\ H(3) \end{bmatrix} = \begin{bmatrix} 1 & 1 & 1 & 1 \\ 1 & W^1 & W^2 & W^3 \\ 1 & W^2 & W^0 & W^2 \\ 1 & W^3 & W^2 & W^1 \end{bmatrix} \begin{bmatrix} h(0) \\ h(1) \\ h(2) \\ h(3) \end{bmatrix} \quad \dots(4)$$

By bit-reversing the indices of $H(m)$ and by factorizing the matrix of W coefficients into $\log_2 N = 2$ matrices, the above system becomes

$$\begin{bmatrix} H(0) \\ H(2) \\ H(1) \\ H(3) \end{bmatrix} = \begin{bmatrix} 1 & W^0 & 0 & 0 \\ 1 & W^2 & 0 & 0 \\ 0 & 0 & 1 & W^1 \\ 0 & 0 & 1 & W^3 \end{bmatrix} \begin{bmatrix} 1 & 0 & W^0 & 0 \\ 0 & 1 & 0 & W^0 \\ 1 & 0 & W^2 & 0 \\ 0 & 1 & 0 & W^2 \end{bmatrix} \begin{bmatrix} h(0) \\ h(1) \\ h(2) \\ h(3) \end{bmatrix} \quad \dots(5)$$

Finally, because $W^2 = -W^0$ and $W^3 = -W^1$, it follows that

$$\begin{bmatrix} H(0) \\ H(2) \\ H(1) \\ H(3) \end{bmatrix} = \begin{bmatrix} 1 & W^0 & 0 & 0 \\ 1 & -W^0 & 0 & 0 \\ 0 & 0 & 1 & W^1 \\ 0 & 0 & 1 & -W^1 \end{bmatrix} \begin{bmatrix} h_1(0) \\ h_1(1) \\ h_1(2) \\ h_1(3) \end{bmatrix}, \quad \begin{bmatrix} h_1(0) \\ h_1(1) \\ h_1(2) \\ h_1(3) \end{bmatrix} = \begin{bmatrix} 1 & 0 & W^0 & 0 \\ 0 & 1 & 0 & W^0 \\ 1 & 0 & -W^0 & 0 \\ 0 & 1 & 0 & -W^0 \end{bmatrix} \begin{bmatrix} h_1(0) \\ h_1(1) \\ h_1(2) \\ h_1(3) \end{bmatrix} \quad \dots(6)$$

From equation (6), a flowgraph of operations is constructed and shown in Figure: 1.0.

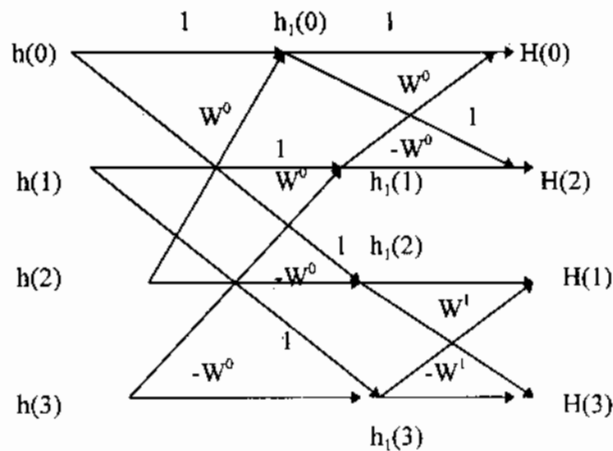


Figure: 1.0 - Flowgraph of FFT operations for $N=4$.

The above figure indicates that not only the number of multiplications is reduced but the number of additions is reduced as well, since each $h_1(k)$ is computed only once and then used for the computations of all $H(m)$ in which it takes part. These are the main reasons that the FFT is much faster than the conventional Fourier transform, see Brigham, (1988).

Dr. Wan Abdul Aziz Wan Mohd. Akib

Dr. Wan Abdul Aziz Wan Mohd. Akib is an Associate Professor in Integrated Geodesy at the Faculty of Engineering and Science Geoinformation, UTM. He graduated in Surveying Sci. from the University of Newcastle Upon-Tyne (UK) in 1980 and University of Queensland Australia in 1985. In 1995, he received a Ph.D degree in Integrated Geodesy from University of London, UK. His research interests comprises several aspects of gravity field modelling and GPS.